

HEAT LOADS ANALYSIS AND CREATION OF A UNIFORM MODEL FOR COMMERCIAL REFRIGERATION EQUIPMENT CALCULATION

Ivan Konstantinov

Department of Refrigeration and Air-Conditioning¹

Mykhailo Khmelniuk

Department of Refrigeration and Air-Conditioning¹

Oleksii Ostapenko✉

Department of Refrigeration and Air-Conditioning¹
ostapenkosc@gmail.com

Ruslan Talibli

Department of Refrigeration and Air-Conditioning¹

Olga Yakovleva

Department of Refrigeration and Air-Conditioning¹

¹*Odessa National University of Technology*
112 Kanatna str., Odessa, Ukraine, 65039

✉ Corresponding author

Abstract

The global commercial refrigeration equipment market size was valued at USD 33.53 billion in 2020. It is expected to expand at a compound annual growth rate (CAGR) of 4.2 % from 2021 to 2028. Furthermore, factors such as regulatory pressures, shift to lower Global Warming Potential (GWP) refrigerants, technological breakthroughs, and the ability to cater to the ever-changing consumer behaviors are also anticipated to create promising growth opportunities for the market. Environmental issues related to high GWP refrigerants, including global warming and ozone depletion, are compelling commercial refrigeration equipment manufacturers to seek alternatives. The rising demand for advancements in technologies that can help reduce hazardous gas emissions has led to the market participants increasingly equipping their products with modern and magnetic refrigeration systems. Apart from this, these systems improve the energy efficiency of refrigeration equipment, bringing down the cost of operation.

The analysis of the structure and heat loads of the commercial freezer with monitoring of temperature distribution on the body of heat-insulating fences and in the internal volume during operation of the system is carried out. The heat loads on the body depending on the structure of the freezer are substantiated on the example of the M400S commercial freezer model. The obtained results allow to significantly reduce the time of selection and calculation of the dimensions of a given model range of equipment for product storage, by developing a standard calculation taking into account the climatic class in which the equipment will be used, and taking into account experimental data obtained during the experiment.

Keywords: refrigeration equipment, temperature distribution, heat loads estimation, low GWP refrigerants.

DOI: 10.21303/2461-4262.2022.001804

1. Introduction

The rapid expansion of the tourism and hospitality sector and the growing preference of end-customers to takeaway meals are expected to emerge as the primary growth factors for the market over the forecast period. A notable increase in international food trade has also triggered the demand for the refrigeration of frozen foods, seafood, and processed foods. With continual innovations, the market has witnessed rapid improvements in technologies such as ammonia absorption systems and liquid-vapor compression. Moreover, the demand for refrigeration equipment has also significantly increased across foodservice industries. To stand out amid competitors, leading manufacturers are emphasizing continual R&D to improve the design and temperature control of their products, among other developments. The need to effectively control and monitor the environment

of a commercial kitchen is anticipated to offer lucrative opportunities to key industry participants in the near future [1–3].

Products offering smart or automated refrigeration controls are finding increased demand in the market. According to the Federal Energy Management Program (FEMP), ENERGY STAR-certified commercial refrigerators consume an average of 1.89 kWh energy per day while lesser efficient refrigerators and freezers consume nearly 4.44 kWh energy per day. The rising demand for energy-efficient commercial refrigerators, thanks to the increased awareness about their cost-effective and environment-friendly nature, is encouraging manufacturers to focus on innovative designs [4–6].

The rapid rise in coronavirus cases globally has compelled the imposition of stringent containment measures, resulting in the slowdown of manufacturing units and reduction in shipments of commercial refrigeration equipment. During these unprecedented times, vaccine storage and handling have, however, become an integral part of the cold storage supply channel to contribute to the effective mass immunization program against COVID-19 [7, 8].

The refrigerators and freezers segment accounted for the highest revenue share of nearly 25 % in 2020 and is anticipated to retain its dominance over the forecast period. The thriving travel and tourism sector globally, which has encouraged the establishment of several food service joints, including restaurants, has contributed to the strong growth of the segment in recent years. The segment also covers blast chillers utilized for promptly freezing or cooling items at lower temperatures and stopping the growth of bacteria in the stored item. The widespread adoption of chillers by healthcare professionals globally, to store tissue samples of controlled tests, vaccines, and critical medicines, is also a key factor contributing to the market growth.

The beverage refrigeration segment is poised to witness the fastest CAGR over the next seven years. The hospitality industry has flourished over the past few years, which has augmented the deployment of medium-capacity personal beverage coolers for travelers and vacationers. Furthermore, various retail channels are now encouraging the ‘sip and shop’ and ‘grab and go’ culture to offer a better shopping experience to their consumers. This trend is further expected to drive the demand for beverage refrigeration equipment over the forecast timeframe.

In the development of commercial trade equipment, detailed calculations of the heat load are not performed, and an experimental method of equipment selection is used. This is due to the small size, specificity of heat exchangers, a wide variety of products, drip condensation, and other aspects. All of the above does not significantly complicate the calculation process, so before the approval of any model of equipment in production, it undergoes numerous tests and inspections in different climatic classes. When inspecting the refrigeration system, it should be noted that the role of the throttle device in commercial low-temperature refrigerators is a capillary tube, the selection of which also entails a number of problems. At the moment, there is a large number of different software for the selection of capillary tubes, but none of them provides information on the required bandwidth of the device, but only offers an approximate length of the tube based on the range of internal diameter. Depending on the manufacturer, the physical properties of the tube, such as roughness or wear resistance, vary, and therefore the information offered by such programs differs from the actual test results. Another significant disadvantage of this product is the placement of the main heat exchangers [9].

2. Materials and methods

2. 1. Research object

The study was conducted at the research site of Yuka-Invest LLC and Odessa National Academy of Food Technologies, Refrigeration and Air-Conditioning department which is equipped with a modern data monitoring system. Climatic conditions in the laboratory are supported by a two-channel ventilation system which includes a humidifier, electric heaters and refrigeration systems [10]. The GECCO system is used for equipment control and data processing. To collect information, a commercial freezer model M400S+ was used (**Fig. 1**). Noting the features of the refrigeration system, it should be noted that it possesses all the necessary features and properties of the M400 model range and has the following characteristics:

- Refrigerant R404A;
- Rated compressor power – 240 W;

- Condenser sizing (length and diameter): 22×0.0047 m;
- Evaporator sizing (length and diameter): 28.8×0.008 m;
- Capillary tube: 3.3×0.0009 m;
- Supercooler sizing (length and diameter): 4.36×0.0047 m.

This model is designed to work in the third climate class at an ambient temperature of 25°C and humidity 60 %. The compressor compartment of the freezer can be removed, which allows to increase the cooled volume, which increases the heat transfer area.

This type of product has six different types of «crown» (straight horizontal, straight beveled, U-shaped horizontal, U-shaped beveled, deaf horizontal cover, deaf beveled cover), which differ in shape and size. Since glass doors have a radial shape, and it is impossible to determine the radius by research without a proper tool, the calculation of their area is performed as the calculation of two legs of an isosceles triangle [11–13]. The inaccuracy of this solution is 2–3 %.

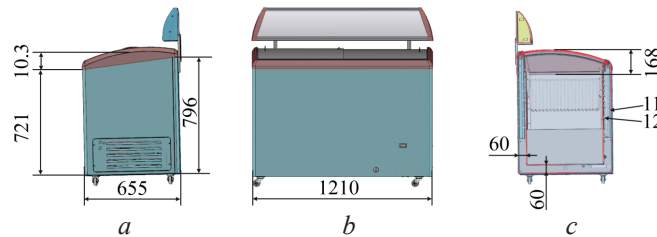


Fig. 1. Freezer model M400S+:

a – side view; *b* – front view with glass cover; *c* – side view with bucket placement

Also, the following data were taken into account, which were found during the study and have a significant impact on the final results: Since the freezer condenser is located on the outside of the housing, the wall temperature in the condenser zone, so in these areas the temperature will be close to the arithmetic mean between ambient temperature and condensation temperature, and the temperature on the compressor side will be $2\text{--}5^\circ\text{C}$ higher than the temperatures on other walls due to the temperature of the compressor and precapacitor. Due to the structure of the compressor compartment and the intensive movement of air, the temperature of the outer part of the bottom will not be uniform, and will decrease along the length of the freezer. Because the compressor compartment has an impeller motor to remove heat from the precapacitor and cool the compressor, the temperature in this volume will be much higher. The temperature in the chamber corresponds to the storage temperature of the product. Most freezers are designed to store frozen product (ice cream, quick-frozen vegetables and fruits, semi-finished products, etc.) and meet the temperature range $-18\text{...}-24^\circ\text{C}$. In general, the heat load from the product is neglected, as it is considered that the product is loaded chilled to the storage temperature and most tests are performed without products. When considering the structure of the chamber, taking into account the location of the container, it was found that the volume of air between the glass and the loading line is a heat-insulating layer, so the heat flow will be calculated as heat transfer from air to products and will be determined by height from the freezer [14–18].

2. 2. Experimental procedures

Since the window has a radial glass door placed at an angle, it was decided to place on the area of the glass panel (sliding door) 12 temperature sensors to determine the dependence of temperature changes on the height of the glass radius to determine the average temperature. The results of the analysis revealed a maximum temperature difference of up to 6.7°C . This indicates the dependence of temperature on the height of the location of the sensitive element on the glass during the natural movement of air in the chamber.

Based on the structure of the freezer and the location of the condenser winding, it was found that in the area of the condenser the temperature on the housing will be much higher than the ambient temperature. However due to the constructional specifics of the freezer and compact placement of the condenser relatively to evaporator the heat transfer takes its place [19, 20]. Considering

the location of the components of the refrigeration system in the compressor compartment, it is possible to conclude that due to heat inflows from the heat exchanger to remove overheating and the compressor, the temperature in the compressor compartment will be much higher and due to dynamic air movement equal in all areas.

During the experiment, temperature sensors were placed along the height of the chest, fixed with aluminum tape HPX ALU/PET50100 at a distance of 100 mm and insulated from external heat with insulating rubber tape Insul 50*3 mm. The dependence of temperature change on time is shown in Fig. 2. When inspecting the design of the freezer, it should be noted that all freezers of this type are fitted with wheels or support legs. Given this feature, and the possibility of air circulation between the compressor compartment and the volume of air under the chest, it is possible to predict that the temperature of the outer part of the bottom will be uneven and will decrease along the length of the freezer, Fig. 3.

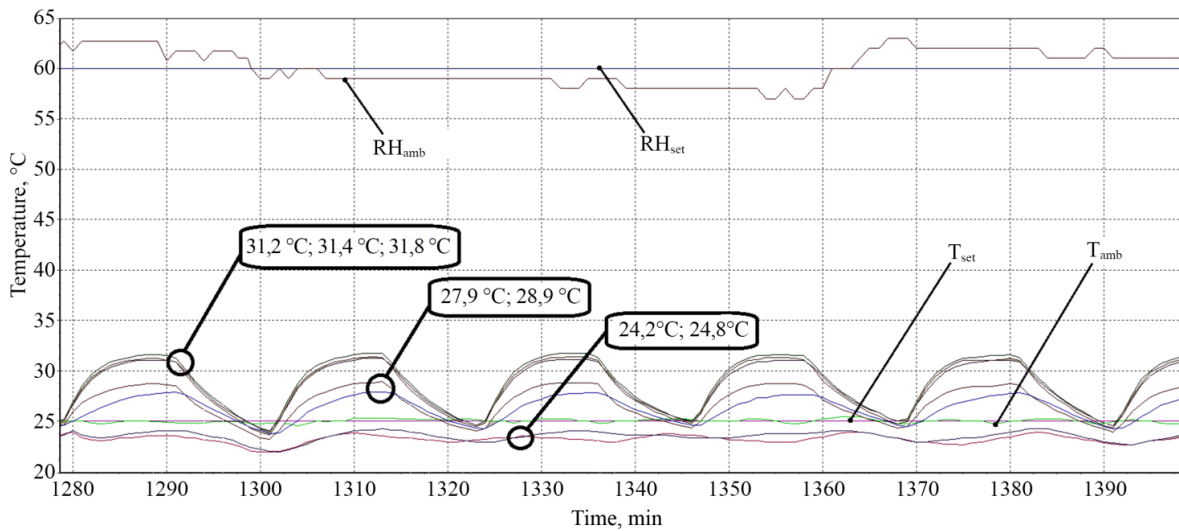


Fig. 2. Temperature and time dependence for sensors located on the freezer housing and in a compressor compartment. Where: RH_{amb} – humidity of the environment; RH_{set} – set ambient humidity; T_{amb} – ambient temperature; T_{set} – set ambient temperature

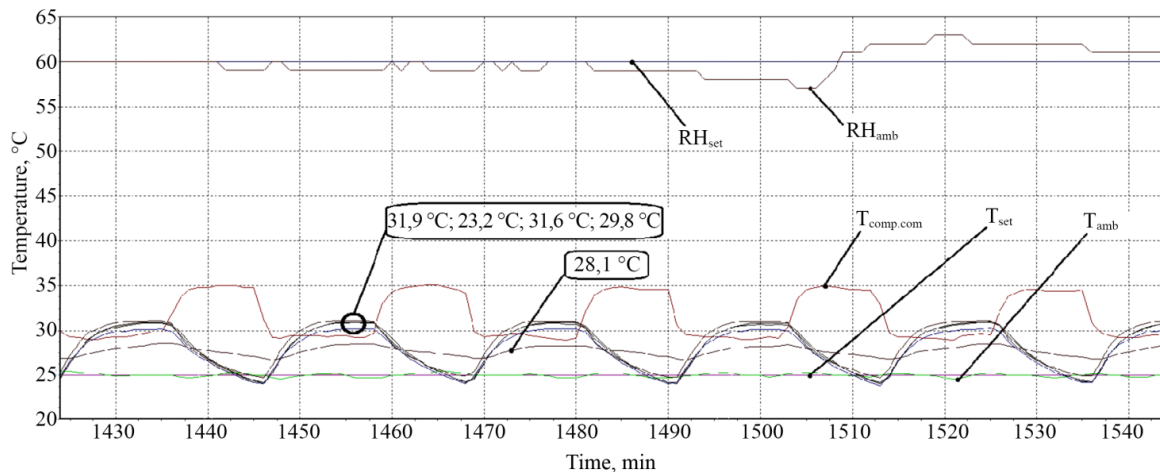


Fig. 3. Temperature and time dependence for sensors located on the freezer housing and in a compressor compartment. Where: RH_{amb} – humidity of the environment; RH_{set} – set ambient humidity; T_{amb} – ambient temperature; T_{set} – set ambient temperature

The test was performed similarly to the measurement of heat load on the body, the results are shown graphically in Fig. 4.

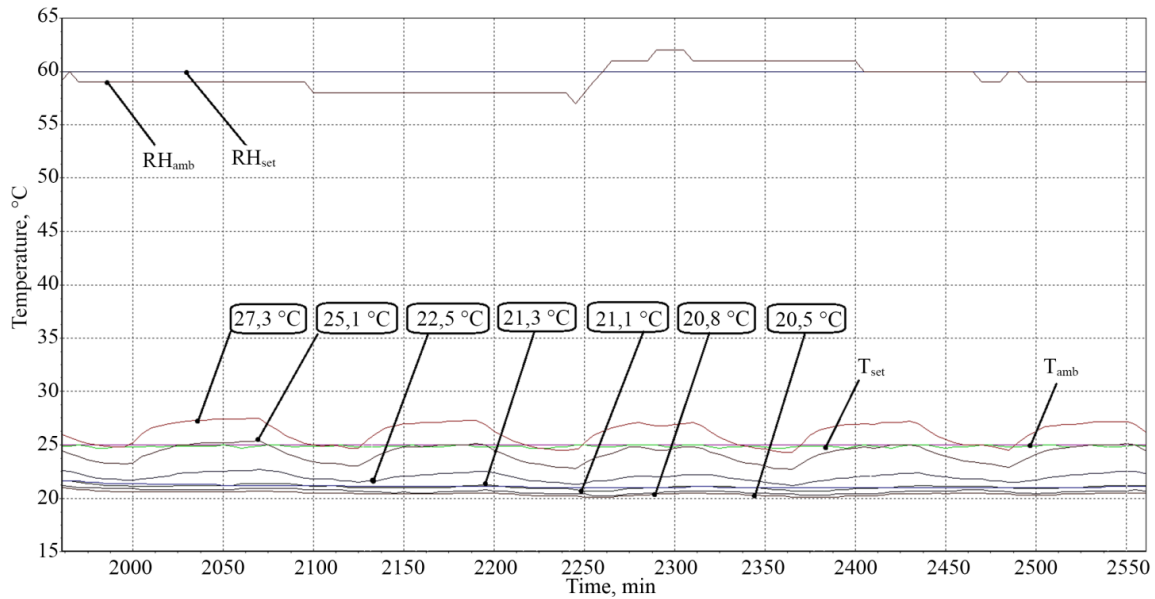


Fig. 4. Temperature – time graph for sensors at the bottom of the refrigerated volume.
 RH_{amb} – humidity of the environment; RH_{set} – set ambient humidity; T_{amb} – ambient temperature;
 T_{set} – set ambient temperature

Given the specification of the sheet-tube evaporator, it was decided to take temperature measurements on the area of this heat exchanger and graphically show the temperature differences in the height of the evaporator **Fig. 5, 6**.

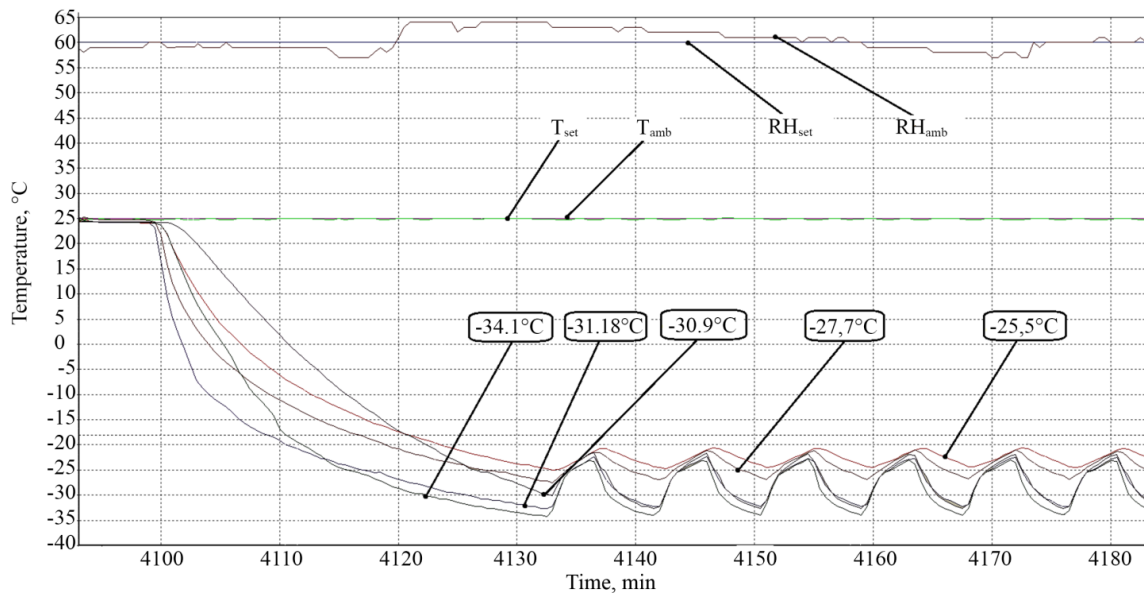


Fig. 5. Temperature – time graph for sensors of the cooled volume temperature

Based on **Fig. 7**, the lower air temperature in the lower part is justified by the natural (gravitational) movement of air in the middle of the chamber.

The higher temperature at the location of the container is justified by additional heat inflows from the «baskets».

The highest temperature at the level of the «crown» confirms that the «dead volume» is a heat-insulating layer.

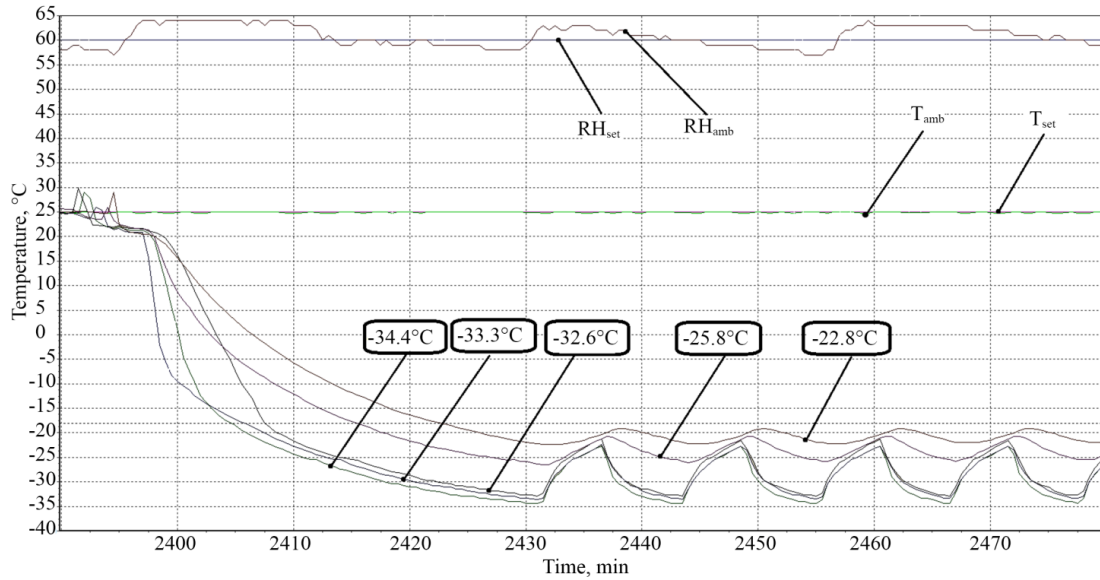


Fig. 6. Temperature – time graph for sensors of the cooled volume temperature.
Where RH_{amb} – humidity of the environment; RH_{set} – set ambient humidity;
 T_{amb} – ambient temperature; T_{set} – set ambient temperature

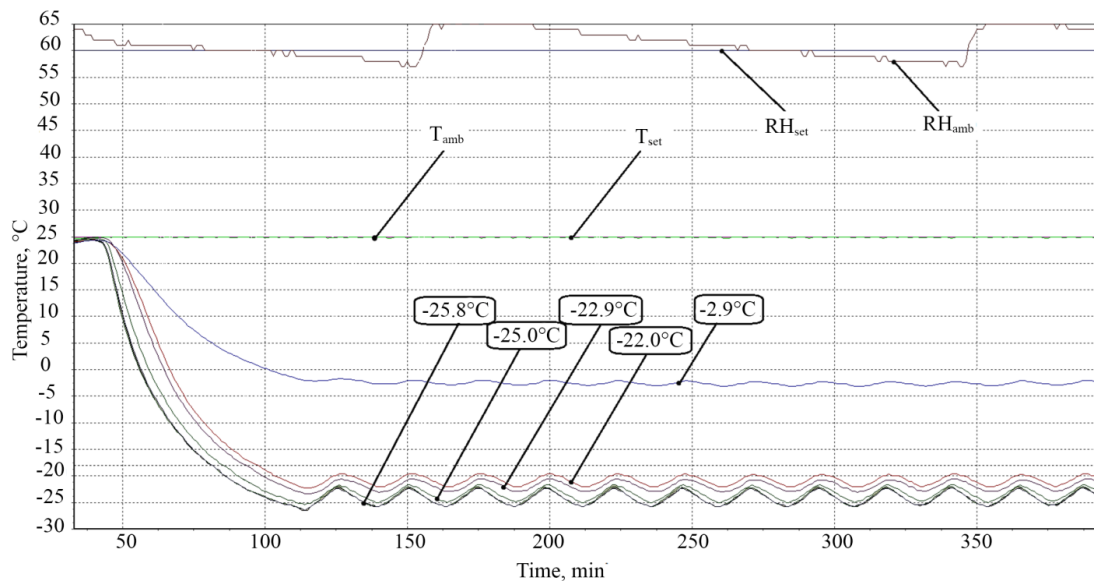


Fig. 7. Temperatures in the refrigerated volume depending on the cooling time.
Where RH_{amb} – humidity of the environment; RH_{set} – set ambient humidity;
 T_{amb} – ambient temperature; T_{set} – set ambient temperature

3. Results and discussion

After conducting experimental measurements, the following results were obtained, which can be taken into account in the thermal calculation to determine the optimal dimensions of a number of models of freezers. Due to the peculiarities of the structure and the results of experimental experiments, a change in temperature along the height of the cooled volume of the freezer was detected, so the temperature difference (1) takes the form:

$$\Delta t = \frac{t_c + t_{amb}}{2} - t_{cv}, \quad (1)$$

where t_c – the condensation temperature is accepted; t_{amb} – ambient temperature; t_{cv} – temperature in the cooled volume.

K_{ins} – in this equation is taken as the sum of heat transfer coefficients (2) through all areas of thermal insulation:

$$K_{ins} = \sum K_{ins}^n. \quad (2)$$

Experimentally, when considering the range of products of freezers, it was found that the free zone of the condenser is 49 %. Therefore, the formula (3) for calculating the area of heat flow through the freezer walls has the form:

$$S_w = \sum S_w \cdot 0.49, \quad (3)$$

where $\sum S_w$ – total area of horizontal walls.

The final form of the formula for calculating the heat flow through the barrier (4) has the form:

$$Q_w = \sum K_w^n \cdot (\sum S_w \cdot 0.49) \cdot \left(\frac{t_k + t_{amb}}{2} - t_{cv} \right). \quad (4)$$

Since it is experimentally proved that the temperatures along the bottom of the chest, due to design features change, the calculation (5) was carried out similarly to the thermal calculation through the barrier:

$$Q_b = \sum K_b^n \cdot \sum S_b \cdot \left(\frac{t_k + t_b}{2} - t_b \right). \quad (5)$$

It is experimentally determined that the temperature in the compressor compartment averages 145 % of the ambient temperature:

$$Q_{load} = \sum K_{load}^n \cdot \sum S_{load} \cdot (t_{amb} \cdot 1.45 - t_{cv}). \quad (6)$$

This heat load is the heat inflow from the top of the freezer, given the principle of temperature distribution in the cooled volume, the value of heat inflow is relatively small, the formula for calculating heat inflow through glass and dead volume (7):

$$Q_g = K_g \cdot S_g \cdot (t_{amb} - t_{cv}). \quad (7)$$

Since the freezer is not a sealed system, and cold air has a larger mass, heat transfer due to convection is taken as 5 % of heat inflow through all insulating surfaces of the cooled volume,

$$Q_{a.v} = \sum Q \cdot 0.05. \quad (8)$$

These heat inflows include 3–8 % of the sum of heat inflows through the insulating surfaces and the thermal load due to the movement of air,

$$Q_u = (\sum Q_{surfaces} + Q_{a.v}) \cdot 0.05. \quad (9)$$

The formula for calculating the heat load from the container is as follows:

$$Q_{tare} = c_{tare} \cdot m_{tare} \cdot \Delta t_{tare}, \quad (10)$$

here c_{tare} – heat capacity of container material, m_{tare} – table tare, Δt_{tare} – the temperature difference from the beginning of cooling to the final temperature.

The coefficient of the mass of the container, determined experimentally and is the mass of the container per unit length of the chest (11):

$$m_{tare} = 5.366 \cdot L_{inner}. \quad (11)$$

The heat load from the product is calculated depending on the weight of the product in the volume of the freezer (12):

$$Q_{pr} = C_{pr} \cdot m_{pr} \cdot \Delta t_{pr}, \quad (12)$$

where C_{pr} – heat capacity of the product; m_{pr} – product weight; Δt_{pr} – the difference between the temperature in the chamber and the temperature of the product.

The weight of the product (13) depends on the percentage of download therefore:

$$m = V_{useful} \cdot \rho_{pr} \cdot \%_{load}. \quad (13)$$

The total load on the evaporator from the product and packaging depends on the time required for entering the mode (14), so:

$$Q_{load} = (Q_{pr} + Q_{tare}) \cdot \frac{t_{amb} \cdot 0.1}{\tau_{req}}. \quad (14)$$

Total heat inflow (15) is determined by the formula:

$$Q_{total} = Q_{cond.zone} + Q_{load} + Q_g + Q_{cov} + Q_{a.v} + Q_u + Q_{load} + Q. \quad (15)$$

When performing several calculations, the difference between the two calculations is not more than 5 %, and it is accepted to take the compressor power by the arithmetic mean between the two calculations. The rated power of the compressor is 0.230 kW. On the refrigerator of the M400S+ model the compressor of the Embraco EMT2130GK model its power makes 0.240 kW at the given temperature conditions is established.

All calculated heat inflows are summarized in **Table 1**. The difference is about 5 % so the calculation is accepted as correct.

Mass of refrigerant circulating in the system (16):

$$\sum M = (V_{ref}^s + V_{ref}^d) \cdot \rho_{ref}, \quad (16)$$

where V_{ref}^s – Refrigerant volume on the suction line; V_{ref}^d – Refrigerant volume on the discharge line.

Table 1
Heat inflows

Heat inflows, W									
Q cond. zone	Q side walls	Q bottom	Q step	Q glass	Q crown	Q air volume	Q unaccounted	Q product and tare	ΣQ
52.6	22.85	13.61	8.69	16.77	14.3	6.44	6.76	13.63	155.62

The result of this experiment is the confirmation of the additional heat load on the cooled volume from the condenser and the compressor compartment (**Table 1**), and the selection of heat through the insulation of the housing. The experiment was performed for the 5.85 kg of product loaded to the freezer. The obtained experimental results confirm the non-uniformity of heat load distribution over all areas of the freezer due to the design features of the unit and allow to calculate the heat load on the evaporator by the zonal method.

Experimental results were obtained in test facility with optimal heat load and constant ambient temperature in the room. These conditions were taken as reference, as they correlate with 80 % of the equipment users. Our next goal is to test the stress conditions with exceeding heat load and higher ambient temperature which is comparable to southern region conditions.

4. Conclusions

Experiments and calculations allow quickly and accurately calculate 12 different options for a freezer with different volume, taking into account climatic classes. Graphical representation of temperatures distribution in the freezer volume shows areas of increased heat load. The overall result of the experiments makes it possible to develop and calculate the total heat input to the cooled volume of the freezer. The obtained results revealed an error of up to 10 % of the existing prototypes. Which allows today to use the calculation model during the manufacture of experimental models of commercial equipment.

Proposed heat load model was developed to calculate new and existing equipment, which makes it easier to make improvements at design stage and minimize future costs. Experimental results have proven its feasibility and applicability for new equipment and for retrofitting the existing units.

References

- [1] Gowreesunke, B. L., Tassou, S. A., Raeisi, A. H. (2014). Numerical study of the thermal performance of well freezer cabinets. 3rd IIR International Conference on Sustainability and the Cold Chain. London. Available at: https://www.researchgate.net/publication/288649461_Numerical_study_of_the_thermal_performance_of_well_freezer_cabinets
- [2] Suamir, I. N., Rasta, I. M. (2019). Studi Eksperimental Kinerja Temperatur dan Energi Integrasi Bio-PCM Pada Chest Freezer. Matrix : Jurnal Manajemen Teknologi dan Informatika, 9 (1). doi: <https://doi.org/10.31940/matrix.v9i1.1046>
- [3] Doiphode, P., Tendolkar, M., Balan, P. A., Samanta, I. (2014). Numerical analysis of chest freezer's condensing unit. International Journal of Air-Conditioning and Refrigeration, 22 (04). doi: <https://doi.org/10.1142/s201013251450028x>
- [4] Harrington, L., Aye, L., Fuller, B. (2018). Impact of room temperature on energy consumption of household refrigerators: Lessons from analysis of field and laboratory data. Applied Energy, 211, 346–357. doi: <https://doi.org/10.1016/j.apenergy.2017.11.060>
- [5] Li, B., Guo, J., Xia, J., Wei, X., Shen, H., Cao, Y. et. al. (2020). Temperature Distribution in Insulated Temperature-Controlled Container by Numerical Simulation. Energies, 13 (18), 4765. doi: <https://doi.org/10.3390/en13184765>
- [6] Commercial Refrigeration Equipment Market Size, Share & Trends Analysis Report By Product, By Application, By System Type (Self-contained, Remotely Operated), By Capacity, By Region, And Segment Forecasts, 2022–2030. Available at: <https://www.grandviewresearch.com/industry-analysis/commercial-refrigeration-equipment-market>
- [7] Tagliafico, L. A., Scarpa, F., Tagliafico, G. (2012). A compact dynamic model for household vapor compression refrigerated systems. Applied Thermal Engineering, 35, 1–8. doi: <https://doi.org/10.1016/j.applthermaleng.2011.08.005>
- [8] Kalyani Radha, K., Naga Sarada, S., Rajagopal, K. (2012). Development of a Chest Freezer – Optimum Design of an Evaporator Coil. International Journal of Automotive and Mechanical Engineering, 5, 597–611. doi: <https://doi.org/10.15282/ijame.5.2012.6.0047>
- [9] Biglia, A., Gemmill, A. J., Foster, H. J., Evans, J. A. (2018). Temperature and energy performance of domestic cold appliances in households in England. International Journal of Refrigeration, 87, 172–184. doi: <https://doi.org/10.1016/j.ijrefrig.2017.10.022>
- [10] Marques, A. C., Davies, G. F., Maidment, G. G., Evans, J. A., Wood, I. D. (2014). Novel design and performance enhancement of domestic refrigerators with thermal storage. Applied Thermal Engineering, 63 (2), 511–519. doi: <https://doi.org/10.1016/j.applthermaleng.2013.11.043>
- [11] Burgess, T. S. (2015). The Effects Of External Temperature On The Energy Consumption Of Household Refrigerator freezers And Freezers. A&M University. Available at: <https://oaktrust.library.tamu.edu/bitstream/handle/1969.1/155467/BURGESS-THESIS-2015.pdf?sequence=1>
- [12] Dall'Alba, C. C. S., Knabben, F. T., Espíndola, R. S., Hermes, C. J. L. (2021). Heat transfer interactions between skin-type condensers and evaporators and their effect on the energy consumption of dual-skin chest-freezers. Applied Thermal Engineering, 183, 116200. doi: <https://doi.org/10.1016/j.applthermaleng.2020.116200>
- [13] Björk, E. (2012). Energy Efficiency Improvements in Household Refrigeration Cooling Systems. Royal Institute of Technology. Available at: <http://kth.diva-portal.org/smash/record.jsf?pid=diva2%3A514733&dsid=-8483>
- [14] Raeisi, A. H., Suamir, I. N., Tassou, S. A. (2013). Energy storage in freezer cabinets using phase change materials. 2nd IIR International Conference on Sustainability and the Cold Chain. Paris. Available at: <https://iifir.org/en/fridoc/energy-storage-in-freezer-cabinets-using-phase-change-materials-29324>
- [15] ISO 23953-1:2015(en). Refrigerated display cabinets – Part 1: Vocabulary. Available at: <https://www.iso.org/obp/ui/#iso:std:iso:23953-1:ed-2:vl:en>

- [16] ISO/DIS 23953-2(en). Refrigerated display cabinets – Part 2: Classification, requirements and test conditions. Available at: <https://www.iso.org/obp/ui/#iso:std:iso:23953:-2:dis:ed-3:v1:en>
- [17] Ahmed, M., Meade, O., Medina, M. A. (2010). Reducing heat transfer across the insulated walls of refrigerated truck trailers by the application of phase change materials. *Energy Conversion and Management*, 51 (3), 383–392. doi: <https://doi.org/10.1016/j.enconman.2009.09.003>
- [18] Defraeye, T., Nicolai, B., Kirkman, W., Moore, S., Niekerk, S. van, Verboven, P., Cronjé, P. (2016). Integral performance evaluation of the fresh-produce cold chain: A case study for ambient loading of citrus in refrigerated containers. *Postharvest Biology and Technology*, 112, 1–13. doi: <https://doi.org/10.1016/j.postharvbio.2015.09.033>
- [19] Cheng, W.-L., Yuan, X.-D. (2013). Numerical analysis of a novel household refrigerator with shape-stabilized PCM (phase change material) heat storage condensers. *Energy*, 59, 265–276. doi: <https://doi.org/10.1016/j.energy.2013.06.045>
- [20] Mercier, S., Villeneuve, S., Mondor, M., Uysal, I. (2017). Time-Temperature Management Along the Food Cold Chain: A Review of Recent Developments. *Comprehensive Reviews in Food Science and Food Safety*, 16 (4), 647–667. doi: <https://doi.org/10.1111/1541-4337.12269>

Received date 11.05.2021

Accepted date 27.05.2022

Published date 30.07.2022

© The Author(s) 2022

This is an open access article
under the Creative Commons CC BY license

How to cite: Konstantinov, I., Khmelniuk, M., Ostapenko, O., Talibli, R., Yakovleva, O. (2022). Heat loads analysis and creation of a uniform model for commercial refrigeration equipment calculation. *EUREKA: Physics and Engineering*, 4, 67–76. <https://doi.org/10.21303/2461-4262.2022.001804>